Tuijin Jishu/Journal of Propulsion Technology
ISSN: 1001-4055
Vol. 44 No. 6 (2023)

Development of Sn/Nio$_3$ and Ce/Nio$_3$ Nanocomposites and Its Application in Waste - Water Treatment

Akshaya Saravanan, Anandalakshmi Haridhass*

Department of Chemistry, Annamalai University, Annamalai Nagar
Mail id : anandhilakshmi74@yahoo.co

Abstract

To synthesis nickel oxide nanocomposites based on tin and cerium, a simple hydrothermal method was employed. The synthesized NiO, Sn/NiO_3, and Ce/NiO_3 nanoparticles were characterized using analytical methods as XRD, FT-IR, SEM, and UV-DRS. The crystalline sizes of NiO, Sn/NiO_3 and Ce/NiO_3 are 29.4, 36.7 and 47.6 nm, respectively. When surface morphologies were investigated using SEM, it was discovered that NiO, Sn/NiO_3 and Ce/NiO_3 nanocomposite showed spherical, agglomerated matrix and irregular structures. The Sn/NiO_3 band gap was 2.5 eV and Ce/NiO_3 was 2.0 eV, respectively, according to the Kubelka-Munk function plot, which was used to determine the band gap using UV-DRS analysis. Using methylene blue dye, we were able to achieve up to 83.2% degradation efficiency property in Ce/NiO_3 nanocomposites through photocatalytic degradation.

Introduction

Environmental pollution has become great issue in recent years. Every day, pollution levels rise, harming the world irreversibly and seriously. Industrial wastewater has been shown to be the main cause of water pollution. One essential step in the treatment of wastewater that might eliminate dangerous heavy organic pollutants is photocatalytic degradation[1]. High separation costs and the secondary creation of pollutants associated with adsorption, clotting, and membrane separation all of which have substantial operating cost are side effects of traditional wastewater treatment applications. Metal oxide nanocomposites enhances photocatalytic degradation when it is present[2]. Researchers in several fields, including photocatalytic performance, gas sensors, glucose sensors and solar cells, are interested in Sn/NiO_3 and Ce/NiO_3 nanostructures. Overall, Ce/NiO_3 metal oxide nanocomposites are more effective photocatalysts.

Because of the environmentally beneficial product, it is becoming progressively more important to develop novel and effective nanocomposite materials. In this study, Sn/NiO_3 and Ce/NiO_3 were used to assess the degradation of methylene blue dye under solar radiation, and the observed data has been analyzed and studied.

Experimental

The required chemicals in this study were Nickel nitrate ($Ni(NO_3)_2$), Tin chloride hexahydrate ($SnCl_2.6H_2O$), Cerium nitrate ($Ce(NO_3)_2$) and Oxalic acid all of which were analytical grade and used without further purification.

Synthesis of Nickel oxide nanoparticles

To perform a one-step hydrothermal synthesis of NiO 2.61g of nickel nitrate trihydrate ($Ni(NO_3)_2.3H_2O$) and 0.24g of the NaOH was added into 70 ml of distilled water and NaOH was added into the solution to maintain the pH value at 7, kept under magnetic stirring for 30 minutes at room temperature[3]. The mixed solution was transferred into a 150 ml Teflon lined stainless steel autoclave heated at 160°C for 10 h. After cooling down to normal temperature, the sample was washed with distilled water and ethanol. The product was dried at 80°C in hot air oven[4].

Synthesis of Sn/NiO_3 nanocomposite

The Sn/NiO_3 nanostructure was synthesized via a typical hydrothermal method. 1.74 g of nickel nitrate trihydrate ($Ni(NO_3)_2.3H_2O$) was added into 40 ml of distilled water and 0.12g of the NaOH were added into the solution to maintain the pH value at 7[5]. The 1.13g of Tin chloride hexahydrate ($SnCl_2.6H_2O$) was added to the reaction mixture. The above mixed solution was maintained at the temperature of 80°C under magnetic stirring for 30 min. The whole solution was transferred into a Teflon lined stainless steel autoclave. The autoclave was kept at 160°C for 10 h. Subsequently, the reaction mixture was allowed to cool at room temperature. The synthesized product was washed with distilled water and ethanol followed by drying at 80°C for overnight and stored for further studies[6].

Synthesis of Ce/NiO_3 nanocomposite

In hydrothermal synthesis of Ce/NiO_3 nanocomposite, 1.74g of nickel nitrate trihydrate ($Ni(NO_3)_2.3H_2O$) was dissolved in 40ml of water and 0.12g of the NaOH was added into 20 ml of distilled water to maintain the pH value at 7, and kept under magnetic stirring for 30 minutes at room temperature. The mixed solution was transferred into a 150 ml Teflon lined stainless steel autoclave heated at 160°C for 10 h. After cooling down to normal temperature, the sample was washed with ethanol and distilled water. The product was dried at 80°C for overnight in a hot air oven[7].

Characterization of NiO, Sn/NiO_3 and Ce/NiO_3 nanocomposite

XRD Analysis

The XRD patterns of the prepared samples after calcination at 500 °C were analysed and the observed diffraction peaks at 2θ values of NiO nanoparticle were found in the planes of (111), (200), (111) and (220), respectively (**JCPDS Card No. 89-5881**)[8]. Sn/NiO_3 nanoparticles are ascribed to the reflection plane of (110), (200) and (311), which matched with **JCPDS Card No. 28-0711**[9]**.** Ce/NiO_3 nanoparticles are ascribed to the corresponding planes of (311), (111), (200) and (220) confirmed the formation and well matched with **JCPDS Card No. 43-1002**[10]. These phenomena indicate that the formation of NiO, Sn/NiO_3 and Ce/NiO_3 nanocomposite began at the calcination temperature of about 450 °C. Peaks are not detected in other phases, indicating the high purity of the products shown in **(Fig.1**). Crystallite size of NiO, Sn/NiO_3 and Ce/NiO_3 nanocomposite were calculated by using Debye–Scherrer formula (Equation 1) and the values were presented in **Table 1.**

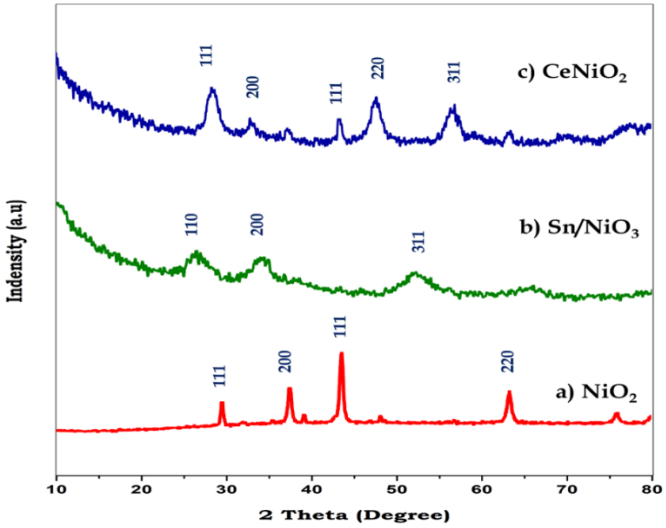

Fig.1 XRD spectra of (a) NiO_2, b) Sn/NiO_3 and (c) $CeNiO_2$ nanoparticles

Debye–Scherer's equation

$$\text{Crystalline size (D)} = \frac{0.9\lambda}{\beta \cos\theta} \quad \text{------ (1)}$$

Where λ is the wavelength (λ = 1.5406 Å (Cu Kα), β is the full width half maximum (FWHM) and θ is the diffraction angle.

Table.1. Crystalline size of NiO, Sn/NiO_3 and Ce/NiO_3 nanocomposite

S.No	Sample	Crystaline Size(nm)
1.	NiO	29.4
2.	Sn/NiO_3	36.7
3.	Ce/NiO_2	47.6

FT-IR Spectrum of NiO, Sn/NiO_3 and Ce/NiO_3 nanocomposite

The FT-IR technique is a strong tool to analyze the different functional groups found in metal oxides, including functional groups involving oxygen. FT-IR spectra of NiO shown in **Fig.2a,** the absorption stretching vibrations peaks are centered at 467 cm^{-1} due to the Ni-O stretching vibrations, the peak of 1346 cm^{-1}[11] which belong to the stretching of C–O and C=O groups presented in the metal oxide nanoparticles and the peak of 3549 cm^{-1} indicates the stretching vibrations of H-O-H. The stretching vibrations peaks of 539 and 523 cm^{-1} are due to the stretching mode of the M-O bond (**Fig.2b and 2**c), 1631 cm^{-1} indicates stretching of C–O and C=O groups presented in the metal oxide nanoparticles[12]. The peak of 3500 and 3486 cm^{-1} indicate the H-O-H stretching vibrations. Since it prevents the combination of charge carriers and also induces a synergistic effect to enhance the catalytic activity of the nanocomposite.

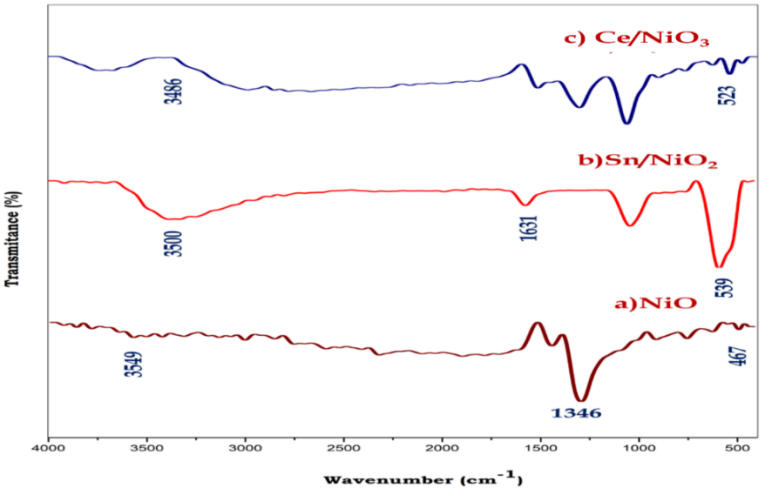

Fig. 2. FT-IR Spectrum of (a) NiO_2, b) Sn/NiO_3 and (c) $CeNiO_2$

Morphology Analysis of NiO, Sn/NiO_3 and Ce/NiO_3 nanocomposite

The surface morphology of the prepared NiO, Sn/NiO_3 and Ce/NiO_3 nanoparticles were analyzed using SEM micrographs and were presented in **Fig.3a and 3b.** The NiO nanoparticle exhibited a agglomerated structure (**Fig.3a**) and the Sn/NiO_3 nanoparticles exhibited an irregular shape **Fig.3b**. Interestingly, Ce/NiO_3 nanoparticles had a spherical shape in different directions[13].

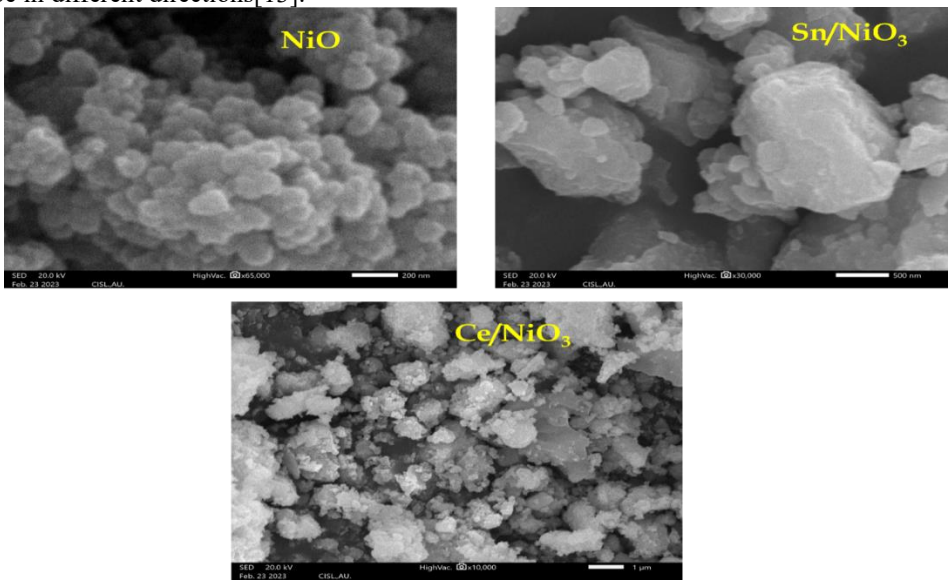

Fig.3 SEM analysis of a)NiO, b)Sn/NiO_3 and c)Ce/NiO_3 nanocomposite

Elemental Analysis of NiO, Sn/NiO_3 and Ce/NiO_3 nanocomposite

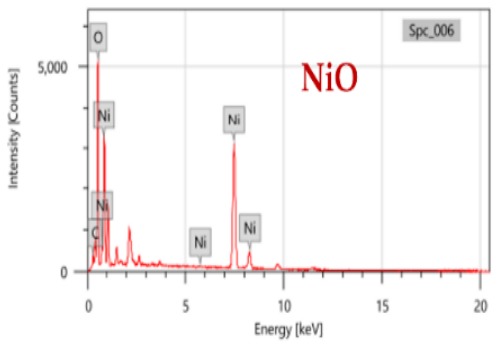

Element	Line	Mass%	Atom%
C	K	5.32±0.08	13.14±0.19
O	K	28.92±0.16	53.62±0.30
Ni	K	65.76±0.39	33.24±0.20
Total		100.00	100.00
Spc_006			Fitting ratio 0.1286

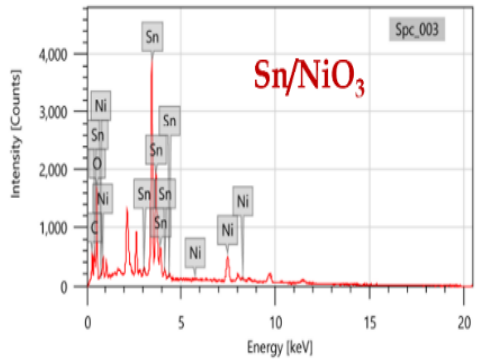

Element	Line	Mass%	Atom%
C	K	3.75±0.04	10.31±0.12
O	K	33.88±0.35	69.89±0.72
Ni	K	8.66±0.15	4.87±0.08
Sn	L	53.71±0.29	14.93±0.08
Total		100.00	100.00
Spc_003			Fitting ratio 0.1882

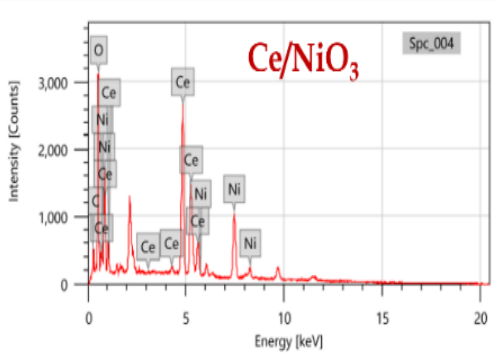

Element	Line	Mass%	Atom%
C	K	3.51±0.04	14.50±0.18
O	K	15.00±0.11	46.58±0.35
Ni	K	20.38±0.22	17.24±0.19
Ce	L	61.12±0.35	21.67±0.13
Total		100.00	100.00
Spc_004			Fitting ratio 0.0848

UV - DRS Analysis of Sn/NiO_3 and Ce/NiO_3 nanocomposite

UV – diffuse reflectance spectroscopy of Sn/NiO_3 and Ce/NiO_3 nanocomposites are shown in **Fig.4** and it was illustrated that pure Sn/NiO_3 and Ce/NiO_3 nanocomposites had significant UV absorption edge observed at 200 to 800nm. But the UV absorption of other samples shifted towards higher wavelength side[14]. The changes in the absorption edges show the changes in the band structure. Further, the bandgap of samples is determined by Kubelka – Munk function equation[15].

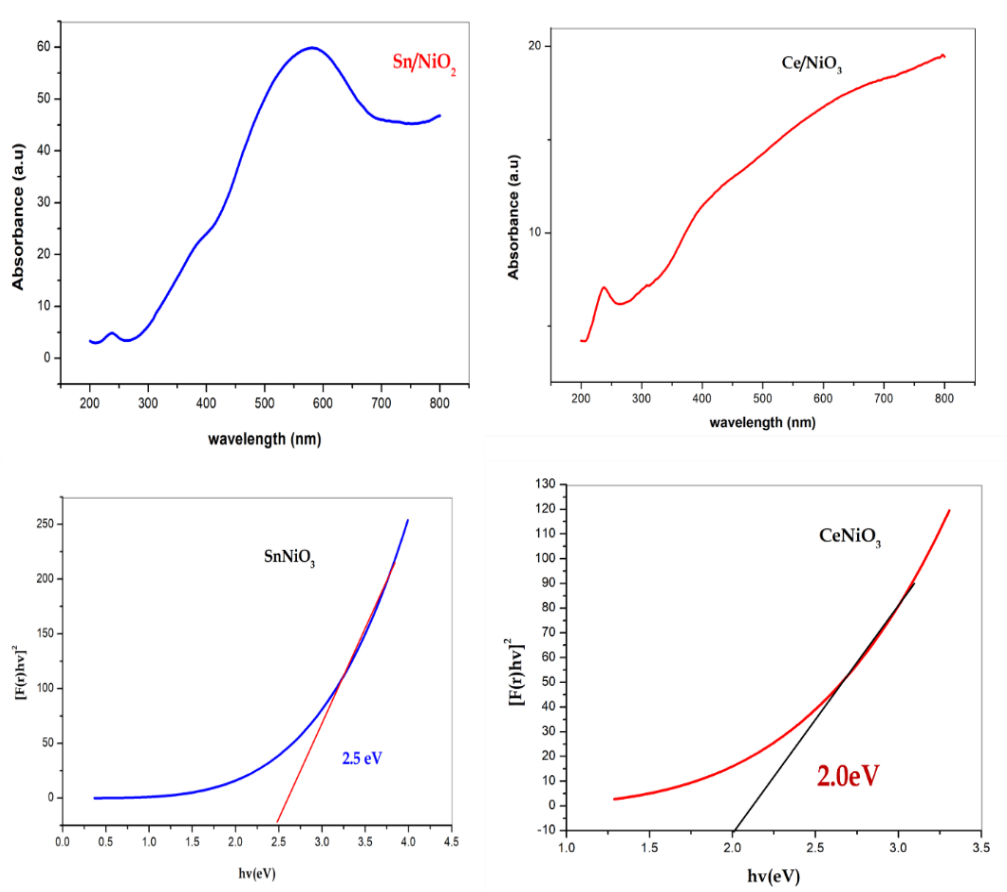

Fig. 4.UV-DRS Image of a) Sn/NiO_3 b) Ce/NiO_3 c) Tauc's plot of Sn/NiO_3 and d) Tauc's plot of Ce/NiO_3

$$\alpha h\nu = A\,(h\nu - E_g)n \quad \text{------ (2)}$$

Where α is the absorption coefficient and hν is the incident photon energy. As shown in **Fig.5**, the bandgap energies are estimated from the intercept of the tangents. The band gap of prepared Sn/NiO_3 and Ce/NiO_3 nanocomposites were found to be 2.5 and 2.0 eV respectively[16]. The presence of oxygen vacancies can create impurity level near the valance bond, so the Ce/NiO_3 has lower band gap value and it is having more catalytic activity compared to the Sn/NiO_3 material.

Photocatalytic Measurements

Photocatalytic activity efficiency of synthesized Sn/NiO_3 and Ce/NiO_3 nanocomposite were evaluated by degradation of methylene blue dye solutions as a model organic pollutant under visible light and sunlight respectively.

The dye degradation using sunlight irradiation was carried out within 60 minutes (**Fig. 5)**. The synthesized Ce/NiO_3 nanocomposite has shown faster dye degradation rate compared with Sn/NiO_3 catalyst[17]. It is evident from **Fig. 5a** that the Sn/NiO_3 nanocomposite has methylene blue degradation efficiency of 72.8%., whereas the Ce/NiO_3 nanocomposite degradation efficiency in methylene blue shows 83.2% within 60 minutes with of sunlight irradiation (**Fig 5b**).

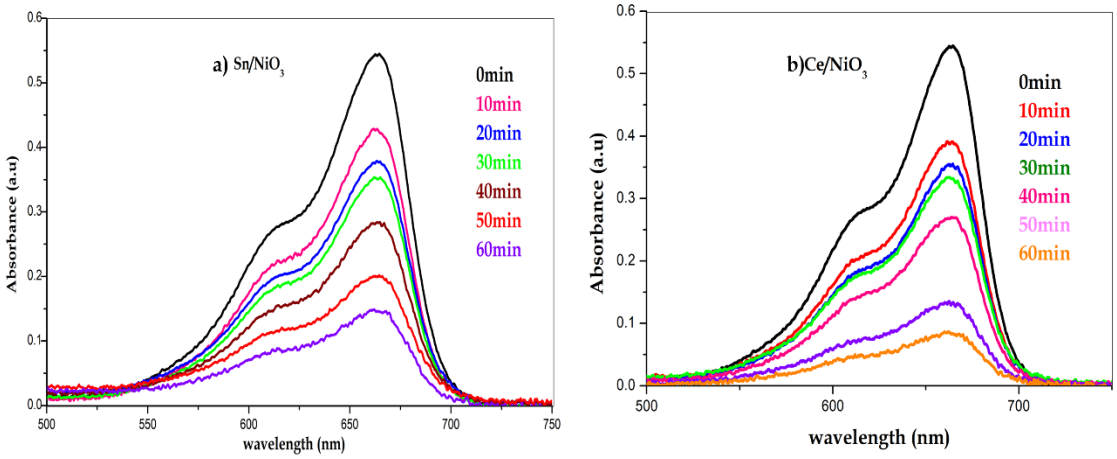

Fig. 5. UV-Vis spectra of a) Sn/NiO_3 and b) Ce/NiO_3 under sunlight irradiation.

The degradation efficiency of the prepared nanocomposites were carried out in 20 mg of the catalyst. **Fig.6a and 6b** explains that the degradation efficiency of the prepared materials by using the sunlight irradiation[18]. Degradation efficiency was recorded in every 10 minutes from which we get the inference that the composite material of Ce/NiO_3 have more efficiency compared to Sn/NiO_3 nanomaterials under the sunlight irradiation.

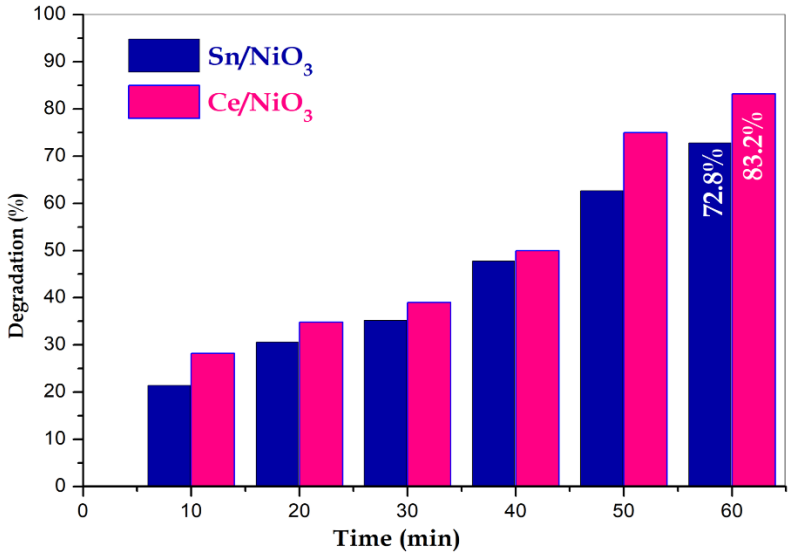

Fig.6. Photocatalytic degradation efficiency of methylene blue dye by using 20mg of catalyst under sunlight irradiation.

Mechanisms of photocatalysis:

When Sn/NiO_3 and Ce/NiO_3 nanoparticles were irradiated with light energy larger than or equal to its band gap energy, conduction band electrons (e^-) and valence band holes (h^+) are produced, according to the actual process of methylene blue dye degradation. The formation of hydroxyl radicals mediates the oxidation of organic compounds, whereas the production of superoxide radicals mediates the reduction and oxidation reactions. Fig.7 illustrates a schematic representation of the degradation mechanism[19]. The hydroxyl radical formed uses the oxidation route to create heterogeneous photocatalysis. The dye might be reduced or the photogenerated by combination of electron with electron acceptors like O_2 adsorbed on the surface or dissolved in water, reducing it to superoxide radical anion $O_2^{\cdot-}$ [20]. The photogenerated holes can oxidize organic compounds by reacting with OH^- or H_2O to produce $^{\cdot}OH$ radicals.

Because the OH radical is such a powerful oxidizing agent, it can oxidize most methylene blue into non-toxic end products such as CO_2, H_2O and mineralized product[21].

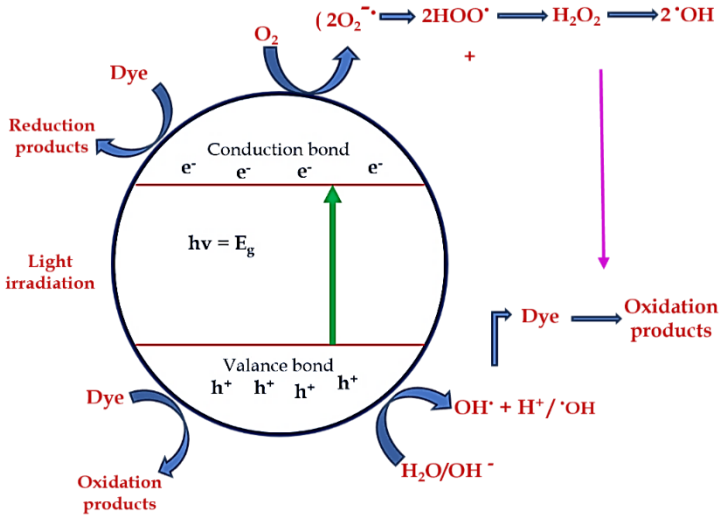

Fig.7. Mechanisms of photodegradation

Conclusion:

The hydrothermal approach was employed to synthesize the nanomaterials viz., Sn/NiO_3 and Ce/NiO_3 and were calcined at 450 °C for 6 hours, producing Sn/NiO_3 and Ce/NiO_3 nanomaterials with a crystalline size of 36.7 and 47.6 nm with the agglomerated matrix and irregular structures. Kubelka - Munk function plot scrutinized that the band gap of Sn/NiO_3 was 2.5 and Ce/NiO_3 was 2.0 eV, respectively. The photocatalytic performance of the synthesized Sn/NiO_3 and Ce/NiO_3 nanocomposites against methylene blue dye was evaluated by sunlight irradiation with 20mg of weight percentages of the catalyst. Ce/NiO_3 nanomaterial showed a high degradation property (83.2%) compared to Sn/NiO_3 materials (72.8%). The sunlight irradiation is a preferable source for eco-friendly photocatalytic degradation processes. The materials were also used for reducing water pollution via an efficient photodegradation processes.

Reference

1. Mohammad, Akbar, et al. "Adsorption promoted visible-light-induced photocatalytic degradation of antibiotic tetracycline by tin oxide/cerium oxide nanocomposite." *Applied Surface Science* 565 (2021): 150337.
2. El Desouky, Fawzy G., M. M. Saadeldin, and I. K. El Zawawi. "Synthesis and tuning the structure, morphological, optical, and photoluminescence properties of heterostructure cerium oxide and tin oxide nanocomposites." *Journal of Luminescence* 241 (2022): 118450.
3. Mishra, Soumya Ranjan, and Md Ahmaruzzaman. "Cerium oxide and its nanocomposites: Structure, synthesis, and wastewater treatment applications." *Materials Today Communications* 28 (2021): 102562.
4. Bagheri, Samira, Ibrahim Khalil, and Nurhidayatullaili Muhd Julkapli. "Cerium (IV) oxide nanocomposites: Catalytic properties and industrial application." *Journal of Rare Earths* 39.2 (2021): 129-139.
5. Mishra, Soumya Ranjan, and Md Ahmaruzzaman. "Cerium oxide and its nanocomposites: Structure, synthesis, and wastewater treatment applications." *Materials Today Communications* 28 (2021): 102562.
6. Li, Peishen, et al. "Controllable synthesis of cerium zirconium oxide nanocomposites and their application for photocatalytic degradation of sulfonamides." *Applied Catalysis B: Environmental* 259 (2019): 118107.
7. Thambidurai, S., et al. "Enhanced bactericidal performance of nickel oxide-zinc oxide nanocomposites synthesized by facile chemical co-precipitation method." *Journal of Alloys and Compounds* 830 (2020): 154642.
8. Barzinjy, Azeez A., et al. "Green and eco-friendly synthesis of Nickel oxide nanoparticles and its photocatalytic activity for methyl orange degradation." *Journal of Materials Science: Materials in Electronics* 31 (2020): 11303-11316.

9. Mou, Jiayou, et al. "Nickel oxide nanoparticle synthesis and photocatalytic applications: evolution from conventional methods to novel microfluidic approaches." *Microfluidics and Nanofluidics* 26.4 (2022): 25.
10. Purkayastha, Moushumi Dutta, et al. "Modelling the photocatalytic behaviour of pn nickel-titanium oxide nanocomposite." *Chemical Engineering Research and Design* 161 (2020): 82-94.
11. Firisa, Soruma Gudina, Guta Gonfa Muleta, and Ahmed Awol Yimer. "Synthesis of Nickel Oxide Nanoparticles and Copper-Doped Nickel Oxide Nanocomposites Using Phytolacca dodecandra L'Herit Leaf Extract and Evaluation of Its Antioxidant and Photocatalytic Activities." *ACS omega* 7.49 (2022): 44720-44732.
12. Al-Zaqri, Nabil, et al. "Green synthesis of nickel oxide nanoparticles and its photocatalytic degradation and antibacterial activity." *Journal of Materials Science: Materials in Electronics* 33.15 (2022): 11864-11880.
13. Wojtyła, Szymon, and Tomasz Baran. "Copper-nickel-oxide nanomaterial for photoelectrochemical hydrogen evolution and photocatalytic degradation of volatile organic compounds." *Materials Research Bulletin* 142 (2021): 111418.
14. Ahsan, Hajra, et al. "Photocatalysis and adsorption kinetics of azo dyes by nanoparticles of nickel oxide and copper oxide and their nanocomposite in an aqueous medium." *PeerJ* 10 (2022): e14358.
15. Kumari, Anjali, and Annu Pandey. "A review on green synthesis of nickel oxide nanoparticles and their photocatalytic activities." *Materials Today: Proceedings* (2023).
16. El-Katori, Emad E., Ensaf Aboul Kasim, and Doaa A. Ali. "Sol–gel synthesis of mesoporous NiO/ZnO heterostructure nanocomposite for photocatalytic and anticorrosive applications in aqueous media." *Colloids and Surfaces A: Physicochemical and Engineering Aspects* 636 (2022): 128153.
17. Sabouri, Zahra, et al. "Green-based bio-synthesis of nickel oxide nanoparticles in Arabic gum and examination of their cytotoxicity, photocatalytic and antibacterial effects." *Green Chemistry Letters and Reviews* 14.2 (2021): 404-414.
18. Mohammed, Salam A., et al. "Synthesis of NiO: V_2O_5 nanocomposite and its photocatalytic efficiency for methyl orange degradation." *Heliyon* 4.3 (2018).
19. Vishaka, E. J., et al. "NiO-CdO nanocomposite for photocatalytic applications." *Materials Today: Proceedings* 68 (2022): 294-298.
20. Fouda, Safaa R., I. S. Yahia, and Mai SA Hussien. "Photocatalytic degradation of methylene blue and rhodamine B using one-pot synthesized nickel oxide grafted glycine (NiO@ GLY) nanostructured: Oxygen vacancies effect." *Journal of Photochemistry and Photobiology A: Chemistry* 439 (2023): 114622.
21. Rafiq, Sabeera, et al. "Optimization studies for nickel oxide/tin oxide (NiO/Xg SnO_2, X: 0.5, 1) based heterostructured composites to design high-performance supercapacitor electrode." *Physica B: Condensed Matter* 638 (2022): 413931.